Cell

# Sorting of *Drosophila* Small Silencing RNAs

Yukihide Tomari,[1,2,*] Tingting Du,[1] and Phillip D. Zamore[1,*]
[1] Department of Biochemistry and Molecular Pharmacology, University of Massachusetts Medical School, Worcester, MA 01605, USA
[2] Institute of Molecular and Cellular Biosciences, The University of Tokyo, Bunkyo-ku, Tokyo, 113-0032, and PRESTO, Japan Science and Technology Agency, Kawaguchi-shi, Saitama, 332-0012, Japan
*Correspondence: tomari@iam.u-tokyo.ac.jp (Y.T.), phillip.zamore@umassmed.edu (P.D.Z.)
DOI 10.1016/j.cell.2007.05.057

## SUMMARY

In *Drosophila*, small interfering RNAs (siRNAs), which direct RNA interference through the Argonaute protein Ago2, are produced by a biogenesis pathway distinct from microRNAs (miRNAs), which regulate endogenous mRNA expression as guides for Ago1. Here, we report that siRNAs and miRNAs are sorted into Ago1 and Ago2 by pathways independent from the processes that produce these two classes of small RNAs. Such small-RNA sorting reflects the structure of the double-stranded assembly intermediates—the miRNA/miRNA* and siRNA duplexes—from which Argonaute proteins are loaded. We find that the Dcr-2/R2D2 heterodimer acts as a gatekeeper for the assembly of Ago2 complexes, promoting the incorporation of siRNAs and disfavoring miRNAs as loading substrates for *Drosophila* Ago2. A separate mechanism acts in parallel to favor miRNA/miRNA* duplexes and exclude siRNAs from assembly into Ago1 complexes. Thus, in flies small-RNA duplexes are actively sorted into Argonaute-containing complexes according to their intrinsic structures.

## INTRODUCTION

Small interfering RNAs (siRNAs) and microRNAs (miRNAs) play an unexpectedly large role in regulating plant and animal gene expression (Kloosterman and Plasterk, 2006). Twenty-one to twenty-three nucleotides long, these two classes of small silencing RNAs repress the expression of specific genes through mechanistically similar RNA silencing pathways (Baulcombe, 2004; Du and Zamore, 2005; Kim, 2005; Sontheimer, 2005; Tomari and Zamore, 2005). siRNAs are produced by the endonucleolytic cleavage of long, double-stranded RNA (dsRNA) by members of the Dicer family of dsRNA-specific endonucleases (Bernstein et al., 2001). When extensively complementary to their mRNA targets, siRNAs direct cleavage of the phosphodiester bond between the target nucleotides paired to siRNA bases 10 and 11 (Elbashir et al., 2001a; Elbashir et al., 2001b). All known plant miRNAs and at least eight mammalian miRNAs similarly guide cleavage of the mRNAs they regulate (reviewed in Du and Zamore, 2005). In contrast, most animal miRNAs lack sufficient complementarity to guide endonucleolytic cleavage of their regulatory targets. Instead, they promote sequence-specific repression of mRNA translation or accelerate mRNA decay, perhaps by recruiting components of more general mRNA turnover pathways (Valencia-Sanchez et al., 2006).

miRNAs reside in discrete genes and are produced by the sequential processing of long transcripts—pri-miRNAs—by the RNase III enzyme Drosha into pre-miRNAs and of pre-miRNAs by Dicer into miRNA-containing RNA duplexes (Cullen, 2004; Kim, 2005). More than 4000 miRNAs have been reported (Griffiths-Jones et al., 2006), many of which are evolutionally conserved, whereas others are restricted to primates or even to humans (Bentwich et al., 2005; Berezikov et al., 2005, 2006). miRNA are proposed to regulate diverse cellular functions, including developmental timing, cell proliferation, cell death, and fat metabolism. They may also act to make biological regulatory circuits more robust (Stark et al., 2005). miRNA-regulated genes typically contain in their 3′ untranslated regions (UTRs) several partially complementary binding sites for one or more miRNAs (Lewis et al., 2003, 2005; Krek et al., 2005).

Members of the Argonaute (Ago) family of small-RNA-binding proteins lie at the core of all known RNA silencing effector complexes, collectively called RNA-induced silencing complexes (RISCs). RISC variants are distinguished by their Argonaute protein. In *Drosophila*, miRNAs partition between Ago1- and Ago2-RISC (Förstemann et al., 2007 [this issue of *Cell*]), whereas siRNAs associate almost exclusively with Ago2-RISC (Hammond et al., 2001; Okamura et al., 2004). Ago1- and Ago2-RISC are functionally distinct, silencing different types of target RNAs by different mechanisms (Förstemann et al., 2007).

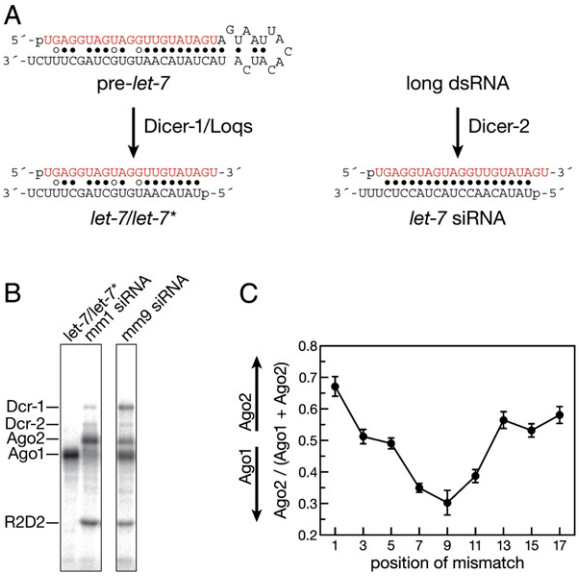


**Figure 1. RNA Duplex Structure Determines the Partitioning of a Small RNA between *Drosophila* Ago1 and Ago2**

(A) A schematic of the distinct small-RNA duplexes produced by Dcr-1 processing of pre-miRNAs and Dcr-2 processing of long dsRNA.

(B) UV crosslinking at 254 nm of exemplary small-RNA duplexes.

(C) A central mismatch directs the duplex into Ago1 instead of Ago2. The fraction of each duplex crosslinked to Ago2 relative to the sum of RNA crosslinked to Ago1 and to Ago2 is presented as the average ± standard deviation for three independent trials.

Both siRNAs and miRNAs are proposed to be loaded into Argonaute protein-containing RISCs from double-stranded intermediates generated by Dicer: siRNA duplexes and miRNA/miRNA* duplexes (Figure 1A). In flies, loading of double-stranded siRNAs into Ago2-RISC is facilitated by the RISC-loading complex (RLC) (Liu et al., 2003, 2006; Pham et al., 2004; Tomari et al., 2004a, 2004b; Pham and Sontheimer, 2005; Kim et al., 2006). The RLC comprises several proteins, including Dicer-2 and its dsRNA-binding partner protein, R2D2. Which strand of the siRNA duplex is assembled into Ago2-RISC is thought to be determined by the orientation of the Dicer-2/R2D2 heterodimer on the siRNA duplex (Tomari et al., 2004a). The strand loaded, the guide strand, typically has a 5′ end less tightly base paired in the duplex than the passenger strand, which is destroyed during the loading process (Khvorova et al., 2003; Schwarz et al., 2003). Passenger-strand destruction and RISC maturation are initiated for Ago2-RISC assembly by guide-strand-directed endonucleolytic cleavage of the passenger strand by Ago2, as if the passenger strand were an mRNA target (Matranga et al., 2005; Rand et al., 2005; Kim et al., 2006; Leuschner et al., 2006). One strand—the miRNA strand—of a miRNA/miRNA* duplex is similarly selectively loaded into Ago1-containing RISC, but the proteins facilitating Ago1 loading remain to be identified (Okamura et al., 2004). Both siRNA and miRNA/miRNA* duplexes contain a ~19 base pair double-stranded core flanked by ~2 nt single-stranded 3′ overhanging ends (Figure 1A). However, the guide and passenger strands of an siRNA duplex are complementary throughout its ~19 bp central domain, whereas the miRNA and miRNA* strands invariably contain G:U wobble pairs, mismatches, and internal loops in this region.

In flies, distinct Dicer complexes produce siRNAs and miRNAs (Lee et al., 2004). miRNAs are cleaved from pre-miRNA by Dicer-1 (Dcr-1), acting with its dsRNA-binding protein partner, Loquacious (Loqs) (Förstemann et al., 2005; Jing et al., 2005; Saito et al., 2005). siRNAs are produced from long dsRNA by Dicer-2 (Dcr-2), which partners with the dsRNA-binding protein R2D2 (Liu et al., 2003). Thus, the different origins of miRNAs and siRNAs might direct them to distinct Argonaute proteins, with Dcr-1/Loqs recruiting Ago1 to miRNAs and Dcr-2/R2D2 directing siRNAs to Ago2. Alternatively, the specific structural differences between a miRNA/miRNA* duplex and an siRNA duplex (Figure 1A) might promote their sorting into Ago1- and Ago2-containing RISC, respectively. Here, we report that the Dcr-2/R2D2 heterodimer acts as a gatekeeper for the assembly of Ago2-RISC, promoting the incorporation of siRNAs and disfavoring the use of miRNAs as loading substrates for *Drosophila* Ago2. An independent mechanism acts in parallel to favor assembly of miRNA/miRNA* duplexes into Ago1-RISC and to exclude siRNAs from incorporation into Ago1. These two pathways compete for loading small-RNA duplexes with structures intermediate between that of an siRNA and a typical miRNA/miRNA* duplex, and such small RNAs partition between Ago1 and Ago2. Thus, small-RNA duplexes are actively sorted into Argonaute-containing complexes according to their intrinsic structures, rather than as a consequence of their distinct biogenesis pathways.

## RESULTS

### A Central Mismatch Favors Small-RNA Loading into Ago1

The structure of a small-RNA duplex could determine into which Argonaute paralog it is loaded. To test this hypothesis, we synthesized ten small-RNA duplexes: an authentic *let-7*/*let-7** duplex; a functionally asymmetric *let-7* siRNA, in which the guide and passenger strands were fully paired except at guide position 1 (mm1 siRNA duplex); and eight *let-7* siRNA duplex derivatives incorporating one additional mismatch between the guide and passenger strands, at guide position 3, 5, 7, 9, 11, 13, 15, or 17 (mm3–mm17 siRNAs) (Figure S1). Each small-RNA duplex, which contained a 5′ $^{32}$P-radiolabel on the *let-7* (guide) strand and a nonradioactive 5′ phosphate on the miRNA* or passenger strand, was incubated in *Drosophila* embryo lysate, then photocrosslinked with 254 nm UV light and analyzed by SDS-PAGE to identify small-RNA-bound proteins. The identity of crosslinked

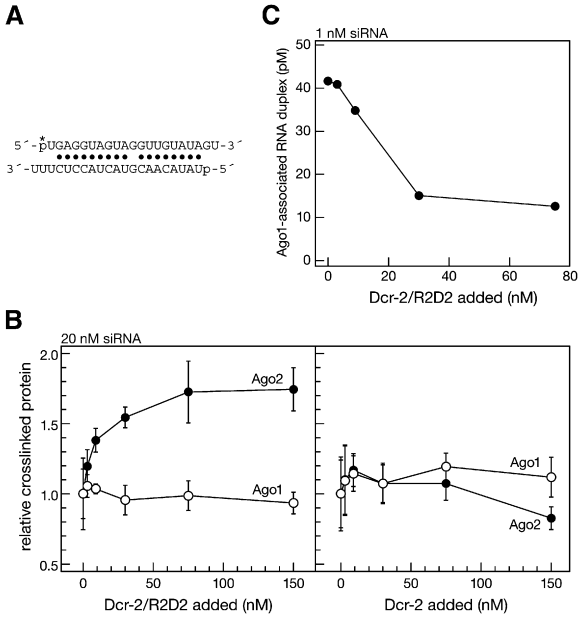


**Figure 2. The Dcr-2/R2D2 Heterodimer, as a Component of the Ago2-Loading Machinery, Promotes Assembly of Ago2-RISC and Competes with Assembly of Ago1-RISC**

(A) Sequence of the small-RNA duplex (mm11) used in (B) and (C).

(B) Dcr-2/R2D2, but not Dcr-2 alone, directs the association of a small-RNA duplex with Ago2. Twenty nanomoles per liter of mm11 duplex, whose *let-7* strand partitions between Ago1 and Ago2, was incubated with wild-type lysate supplemented with increasing amounts of Dcr-2/R2D2 or Dcr-2 alone. Ago1- and Ago2-association were measured by 254 nm UV crosslinking. The data (average ± standard deviation for three trials) were normalized to the crosslinking observed in the absence of supplemental recombinant Dcr-2/R2D2 or Dcr-2 alone.

(C) One nanomoles per liter of mm11 duplex was incubated with wild-type lysate supplemented with increasing concentrations of Dcr-2/R2D2, the Ago1-associated siRNA recovered by immunoprecipitation with anti-Ago1 monoclonal antibody and quantified by scintillation counting.

proteins was assigned by their immunoprecipitation with specific antibodies and their loss in lysate prepared from mutant ovaries or embryos.

The authentic *let-7*/*let-7** duplex crosslinked only to Ago1, whereas the *let-7* mm1 siRNA duplex crosslinked predominantly to Ago2 (Figure 1B). Introducing a position 9 mismatch into the siRNA (mm9) shifted the balance in favor of Ago1, while retaining significant Ago2 association. Quantitative analysis of the ratio of Ago1 to Ago2 crosslinking for the entire series of mismatched *let-7* siRNA derivatives revealed that central mismatches direct small-RNA duplexes into Ago1 rather than Ago2 (Figure 1C).

## A Role for the Dcr-2/R2D2 Heterodimer in Small-RNA Partitioning

How does a central mismatch influence Argonaute loading? Such a disruption to siRNA structure might disfavor its association with the RLC (reducing Ago2 loading), favor its association with the Ago1-loading machinery, or both. To test the idea that central mismatches reduce the association of a small-RNA duplex with the RLC, we incubated a *let-7* siRNA bearing a mismatch at position 11 (mm11) (Figure 2A) with embryo lysate supplemented with purified recombinant Dcr-2/R2D2 heterodimer or Dcr-2 alone. In the absence of supplemental recombinant protein, the mm11 duplex partitioned between Ago1 (~60%) and Ago2 (~40%). Increasing the concentration of the Dcr-2/R2D2 heterodimer, the core constituent of the RLC, increased the amount of duplex crosslinked to Ago2 (Figure 2B). In contrast, increasing the concentration of Dcr-2 alone did not enhance crosslinking of the duplex to Ago2, consistent with earlier observations that R2D2 is required to recruit Dcr-2 to siRNA for RISC loading (Liu et al., 2003, 2006). Moreover, in the absence of R2D2, Dcr-2 reduced Ago2 crosslinking to siRNA (Figure 2B), suggesting that Dcr-2 forms a complex with siRNA that cannot load Ago2 (see below and Figure S2). Together, the data in Figures 1C and 2B suggest that a central mismatch weakens the binding of the Dcr-2/R2D2 heterodimer to a small-RNA duplex, disfavoring its assembly into Ago2-RISC; increasing the concentration of the Dcr-2/R2D2 heterodimer increases loading of the small RNA into Ago2 by overcoming its reduced affinity for the RLC.

## Competition between Ago1 and Ago2 Pathways

Although increasing Dcr-2/R2D2 concentration promoted loading of the mm11 duplex into Ago2, the crosslinking assay cannot determine whether the Ago2- and Ago1-loading pathways compete for loading of an siRNA, because the majority of the 20 nM RNA duplex remained unassociated with the Ago2-loading machinery (Schwarz et al., 2003; Haley and Zamore, 2004). This free RNA creates a reservoir of duplex that can, in principle, be loaded into Ago1. Unfortunately, reducing the concentration of small RNA in the crosslinking assay caused the RNA-crosslinked proteins to become undetectable.

To test if the Ago2- and Ago1-loading pathways compete for loading small-RNA duplexes, we used a lower concentration of small RNA and a more sensitive assay—immunoprecipitation—to measure the association of a small RNA with Ago1. (The assay cannot currently measure small-RNA association with Ago2, because no suitable anti-Ago2 antibody exists.) We incubated 1 nM 5′ $^{32}$P-radiolabeled mm11 duplex in embryo lysate with increasing concentrations of Dcr-2/R2D2, immunoprecipitated Ago1 using a monoclonal anti-Ago1 antibody, and measured the concentration of Ago1-associated small-RNA duplex by scintillation counting. Increasing the concentration of Dcr-2/R2D2 decreased the amount of siRNA associated with Ago1 (Figures 2A and 2C), indicating that Ago1 loading competes with Dcr-2/R2D2-mediated loading of Ago2.

## Measuring the Association of Small RNAs with the Dcr-2/R2D2 Heterodimer

To test directly the idea that the affinity of the Dcr-2/R2D2 heterodimer for a small-RNA duplex determines

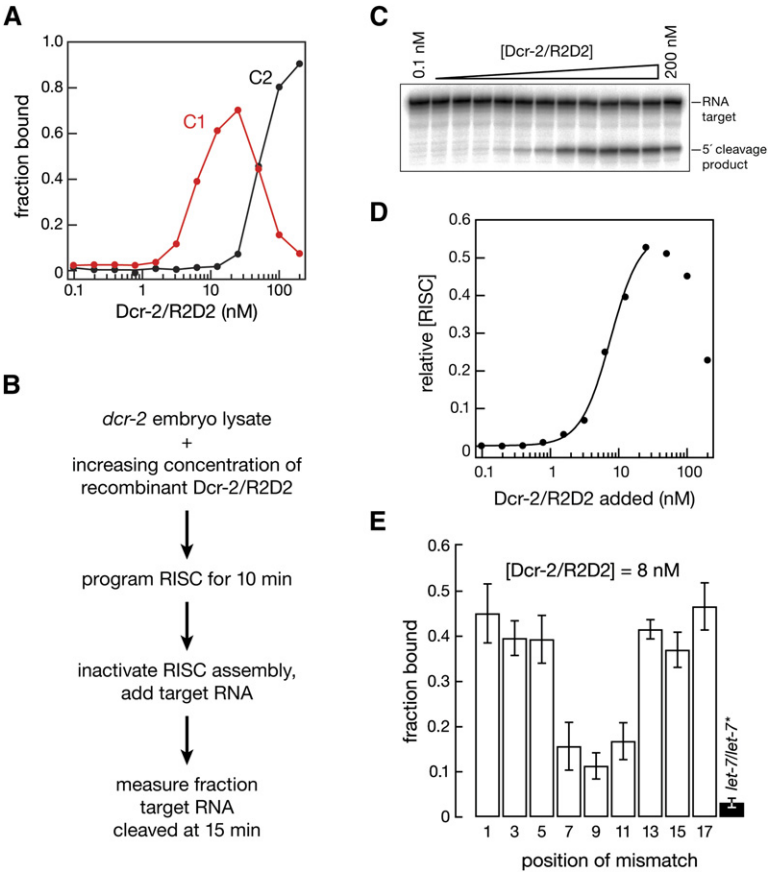


**Figure 3. RISC Activity Coincides with the Formation of Dcr-2/R2D2:siRNA Ternary Complex C1, and a Central Mismatch in a Small-RNA Duplex Impairs the Complex Formation**

(A) Quantification of concentration dependence of the two complexes formed when purified, recombinant Dcr-2/R2D2 heterodimer was incubated with siRNA. The native gel used for this analysis appears in Figure S3A.

(B) Experimental strategy for (C) and (D).

(C) Target cleavage activity was measured for RISC assembled in *dcr-2* mutant lysate—which lacks both Dcr-2 and R2D2—rescued with increasing amounts of recombinant Dcr-2/R2D2 heterodimer.

(D) Quantification of (C). The peak of the target cleavage activity corresponds to the peak of complex C1 formation in (A). The y axis reports the relative concentration of RISC, calculated from a standard curve relating relative RISC concentration to the fraction of target cleaved (Figure S4D).

(E) Each of the ten *let-7* small-RNA duplexes was 5′ $^{32}$P-radiolabled and incubated with 8 nM Dcr-2/R2D2. Then, the fraction of RNA present as complex C1 was measured. No C2 was formed at this concentration of the heterodimer. Bars report the average ± standard deviation for three trials.

the extent of its loading into Ago2-RISC, we used a gel-mobility shift assay to measure the affinity of recombinant Dcr-2/R2D2 heterodimer for the series of ten *let-7* small-RNA duplexes. Purified recombinant Dcr-2/R2D2 and 5′ $^{32}$P-radiolabeled small RNAs bearing a nonradioactive 5′ phosphate on the passenger or miRNA* strand were incubated for 30 min, then free siRNA resolved from protein:siRNA complexes by native gel electrophoresis in the presence of $Mg^{2+}$. Figure S3A shows a representative assay for the *let-7* mm1 siRNA duplex. With increasing concentration of Dcr-2/R2D2, we detected two distinct complexes: complex 1 (C1) peaked at ~20 nM Dcr-2/R2D2, whereas complex 2 (C2) appeared at higher concentrations of Dcr-2/R2D2, apparently replacing C1 (Figures S3A and 3A).

To determine if each complex contained Dcr-2, R2D2, or both, we repeated the assay using a *let-7* siRNA bearing a 5-iodo uracil at guide-strand position 20; 5-iodo U at this position allows the siRNA to be site-specifically photocrosslinked to Dcr-2 or R2D2 upon irradiation with 302 nm light (Tomari et al., 2004a). The *let-7* siRNA was incubated with 20 nM (for C1) or 100 nM Dcr-2/R2D2 (for C2) and photocrosslinked; the complexes were resolved by native gel electrophoresis, and then C1 and C2 were excised from the gel, and the crosslinked proteins in each complex were separated by SDS-PAGE (Figure S3B). Both C1 and C2 contained Dcr-2 and R2D2 crosslinked to siRNA (Figure S3C). Thus, both C1 and C2 reflect binding of the Dcr-2/R2D2 heterodimer to siRNA.

Which complex then corresponds to the active form of siRNA-bound Dcr-2/R2D2 heterodimer competent to load Ago2? We added increasing concentration of recombinant Dcr-2/R2D2 heterodimer to lysate prepared from *dcr-2*$^{L811fsX}$ (Pham et al., 2004) mutant embryos, which lack both Dcr-2 and R2D2 (T.D. and P.D.Z., unpublished data). At each concentration of heterodimer, we measured the relative amount of Ago2-RISC activity assembled by determining the extent of cleavage after 15 min incubation with target RNA (Figures 3B–3D) when the reaction was linear (Figure S4). The Dcr-2/R2D2 concentration producing half-maximal target cleavage in this assay coincided with the apparent dissociation constant ($K_{app}$) for C1 production, indicating that C1 is the active complex for RISC loading (compare Figures 3A and 3D). Interestingly, at high concentrations of Dcr-2/R2D2 heterodimer, which favor the production of C2 (Figure 3A), target cleavage was inhibited (Figure 3D), reinforcing the view that complex C1 is the active, Ago2-loading form of siRNA-bound heterodimer and suggesting that C2 corresponds to a higher order, inactive aggregate of Dcr-2/R2D2 heterodimers.

**Table 1. The Measured and Relative Affinities (± standard deviation) of the Dcr-2/R2D2 Heterodimer for Three Different Small-RNA Duplexes and of Dcr-2 Alone for siRNA**

| Dcr-2/R2D2 Heterodimer | | | |
|---|---|---|---|
| Small RNA | $K_{app}$ (nM) | $K_{relative}$ | Trials |
| *let-7* mm1 siRNA duplex | 7.8 ± 1.2 | 1.0 ± 0.2 | 3 |
| mm9 duplex | 16.3 ± 3.1 | 2.1 ± 0.3 | 3 |
| *let-7*/*let-7** duplex | 37.5 ± 4.6 | 4.8 ± 0.6 | 3 |
| **Dcr-2 Alone** | | | |
| Small RNA | $K_{app}$ (nM) | $K_{relative}$ | Trials |
| *let-7* mm1 siRNA duplex | 94.6 ± 6.4 | 12.1 ± 0.8 | 4 |

## The Affinity of the Dcr-2/R2D2 Heterodimer for a Small RNA Determines Its Loading into Ago2-RISC

Next, we examined the affinity of the Dcr-2/R2D2 heterodimer for various small-RNA duplexes. We measured the $K_{app}$ of the heterodimer for formation of complex C1, the species active for Ago2-loading. Figure S5 (A and B) shows representative binding curves for the mm1 siRNA duplex, mm9 duplex and *let-7*/*let-7** duplex, and Table 1 summarizes the $K_{app}$ for each determined in three independent trials. The Dcr-2/R2D2 heterodimer bound the mm9 duplex about half as tightly as it bound the *let-7* mm1 siRNA duplex, whereas the heterodimer bound the *let-7*/*let-7** duplex about 5-fold less tightly than it bound the corresponding siRNA. Although previous studies concluded that Dcr-2 does not detectably bind siRNA in the absence of R2D2 (Liu et al., 2006), we found that purified recombinant Dcr-2 alone readily bound the mm1 siRNA duplex, with a $K_{app}$ of 94.6 ± 6.4 nM (average of four trials ± standard deviation; Figure S2). Thus, the apparent lack of Dcr-2 binding to siRNA reported previously likely reflects the ~12-fold lower affinity for siRNA of Dcr-2 alone compared to the intact heterodimer.

For the Dcr-2/R2D2 heterodimer, the order of relative affinities of Dcr-2/R2D2 for the three small-RNA duplexes correlated well with their extent of incorporation into Ago1- and Ago2-RISC: the greater the strength of binding of the heterodimer for a small RNA, the greater its association with Ago2 and the more reduced its association with Ago1. To further test this idea, we determined the fraction of small-RNA duplex bound to 8 nM Dcr-2/R2D2 heterodimer for all ten *let-7* small-RNA duplexes (Figure 3E). The amount of small RNA associated with Dcr-2/R2D2 in this assay correlated well with the amount of the small RNA assembled into Ago2 relative to Ago1 (Figures 1B and 1C).

## Small-RNA Association with Ago1 Does Not Ensure the Production of Functional Ago1-RISC

Clearly, the affinity of the Dcr-2/R2D2 heterodimer for a small-RNA duplex is an important determinant of the extent to which the small RNA is loaded into Ago2. Our

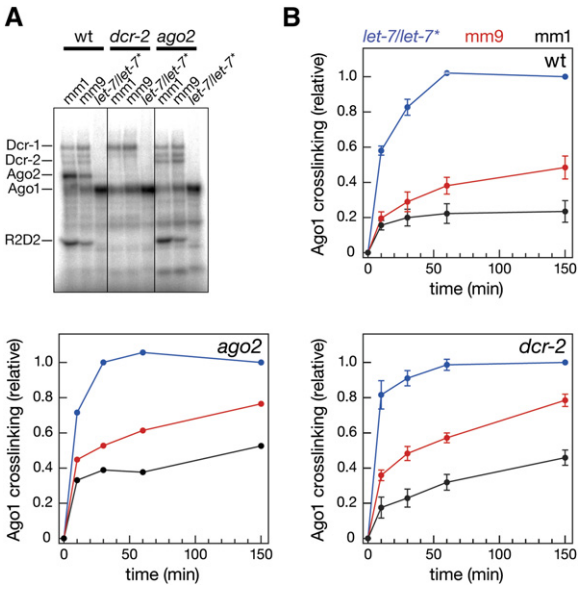


**Figure 4. The Ago1-Loading Pathway Selects Small RNAs with Central Mismatches, Even in the Absence of the Competing Ago2 Pathway**

(A) Three exemplary small-RNA duplexes were incubated with wild-type, *dcr-2*, or *ago2* embryo lysate and then photocrosslinked with shortwave UV to identify small-RNA-bound proteins.

(B) Kinetic analysis of small-RNA association with Ago1, monitored by UV photocrosslinking. The *let-7*/*let-7** duplex associated with Ago1 more rapidly than the mm9 duplex, which was more rapidly bound by Ago1 than the mm1 siRNA duplex. In the absence of the Ago2-loading machinery or Ago2 itself, association of the small-RNA duplexes with Ago1 was accelerated, consistent with the idea that the Ago1 and Ago2 pathways compete for loading with small-RNA duplexes. Each data point represents the average ± standard deviation for three trials.

data also suggest that Ago1 and Ago2 compete for loading with a small-RNA duplex (Figure 2C). In theory, small RNAs whose structure disfavors their loading into Ago2 pathway, might enter the Ago1-loading pathway simply by default. To test this idea, we examined the loading of the mm1 siRNA duplex, mm9 duplex, and *let-7*/*let-7** duplex into Ago1 in lysate prepared from *dcr-2*$^{L811fsX}$ and from *ago2*$^{414}$ mutant embryos. In the *dcr-2*$^{L811fsX}$ and *ago2*$^{414}$ lysates, where Ago2 is not loaded, the relative amount of each small-RNA duplex loaded into Ago1, measured by photocrosslinking, remained essentially unchanged from that observed in wild-type lysate (Figure 4A). Even in the absence of Ago2-loading machinery or Ago2 itself, Ago1 was preferentially loaded with the *let-7*/*let-7** duplex, largely rejected the mm1 siRNA duplex, and accepted some of the mm9 duplex. Thus, both the Ago1- and the Ago2-loading pathways are selective, with each favoring a small-RNA structure disfavored by the other.

While the extent of Ago1 loading was essentially the same in the wild-type and mutant lysates, the rate at which the three small-RNA duplexes associated with Ago1 was

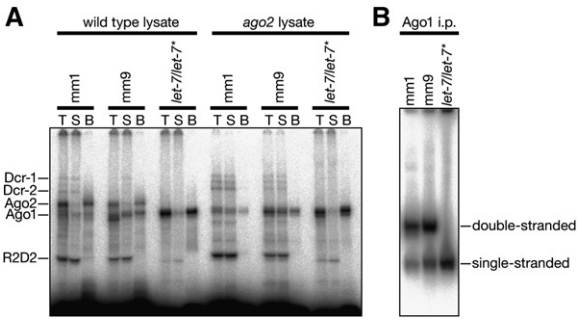


**Figure 5. *let-7/let-7** Duplex, But Not the mm1 siRNA Duplex Nor the mm9 Duplex, Efficiently Assembled Mature Ago1-RISC**

(A) The three exemplary small-RNA duplexes were incubated with wild-type or *ago2* embryo lysate for 1 hr, UV photocrosslinked, and then mature RISC, which contains single-stranded *let-7* RNA, separated from pre-RISC, which contains double-stranded RNA, using an immobilized 2′-*O*-methyl *let-7* ASO. T, total; S, supernatant (double stranded); B, bound (single stranded). The Ago1-associated *let-7* mm1 siRNA duplex and the mm9 duplex remained largely double stranded, suggesting that mature Ago1-RISC was not efficiently formed from the Ago1 pre-RISC assembled with these duplexes. Most of the Ago1-associated *let-7* loaded from the *let-7/let-7** duplex was present as single-stranded *let-7* bound to Ago1. That is, the conversion of *let-7/let-7** Ago1-pre-RISC to *let-7* Ago1-RISC was very efficient. In contrast, the mm1 siRNA duplex and mm9 duplex efficiently loaded single-stranded *let-7* into Ago2; these small-RNA duplexes were efficiently converted from Ago2 pre-RISC to mature Ago2-RISC.

(B) Each small-RNA duplex was incubated with wild-type embryo lysate, the Ago1-associated RNA recovered by immunoprecipitation, and then the small RNA isolated and single-stranded RNA separated from dsRNA by native gel electrophoresis. As in (A), the *let-7* mm1 siRNA duplex and mm9 duplexes produced mainly Ago1-associated double-stranded RNA, whereas the *let-7/let-7** duplex yielded almost entirely Ago1-bound single-stranded *let-7*.

accelerated in both the $ago2^{414}$ and $dcr\text{-}2^{L811fsX}$ lysates (Figure 4B). This effect was most pronounced for the *let-7/let-7** duplex, which was loaded twice as fast in the $dcr\text{-}2^{L811fsX}$ mutant lysate, which lacks the Ago2-loading machinery. The finding that, in the absence of the Ago2-loading machinery, Ago1 is more rapidly loaded with its authentic substrate, the *let-7/let-7** duplex, suggests that miRNA/miRNA* duplexes bind the Dcr-2/R2D2 heterodimer transiently, even when they ultimately make little or no Ago2-RISC.

Conversely, a small-RNA duplex favored to produce Ago2-RISC associated with Ago1 in both the absence and presence of Ago2 (Figures 4A and 4B). But does this Ago1-associated small RNA correspond to mature RISC, which contains only the miRNA or guide strand of the original duplex, or pre-RISC, a RISC-assembly intermediate in which the double-stranded miRNA/miRNA* or siRNA is bound to Argonaute (Matranga et al., 2005; Rand et al., 2005; Kim et al., 2006; Leuschner et al., 2006)? We determined if the *let-7* strand was bound to Ago1 or Ago2 as single-stranded or double-stranded RNA. For the mm1, the mm9 and the *let-7/let-7** duplexes, each 5′-$^{32}$P-radiolabeled small-RNA duplex was incubated with wild-type or $ago2^{414}$ mutant lysate to assemble RISC and photocrosslinked to identify siRNA-associated proteins, and then single-stranded RNA-crosslinked proteins captured using an immobilized 2′-*O*-methyl antisense oligo (ASO) complementary to *let-7* (Figure 5A); in this assay, proteins crosslinked to double-stranded siRNA or miRNA/miRNA* remain in the supernatant. (Dcr-1, Dcr-2, and R2D2 were never recovered with the immobilized ASO, consistent with previous observations that they bind only double-stranded small RNAs [Tomari et al., 2004a)]. As expected, the majority of the crosslinked Ago2 was recovered with the immobilized ASO for the *let-7* mm1 siRNA duplex, whereas most of the crosslinked Ago1 was recovered with the immobilized ASO for the *let-7/let-7** duplex. We conclude that the *let-7* mm1 siRNA duplex efficiently assembled mature Ago2-RISC, whereas the *let-7/let-7** duplex efficiently assembled mature Ago1-RISC. The mm9 duplex also efficiently assembled mature Ago2-RISC.

Much of the Ago1-associated *let-7* loaded from the mm1 siRNA duplex or the mm9 duplex, however, remained double stranded, suggesting that the Ago1-loading machinery or Ago1 itself cannot efficiently dissociate the passenger strand from a highly base paired duplex (Figure 5A). In contrast, little double-stranded, Ago2-associated *let-7* was observed for the mm1 siRNA duplex or mm9 duplex in the wild-type lysate, likely reflecting the rapid cleavage of the passenger strand by Ago2. This is consistent with our findings that Ago1 is not an efficient endonuclease (Förstemann et al., 2007).

We note that in the absence of Ago2, some *let-7*-programmed Ago1-RISC was formed from the mm1 siRNA duplex. The low efficiency of incorporation of the *let-7* siRNA guide strand into mature Ago1-RISC, together with the reduced endonuclease activity of Ago1 compared to Ago2, likely explains the small amount of siRNA-directed target cleavage observed in vitro in lysate prepared from $ago2^{414}$ (Okamura et al., 2004) and $r2d2^{1}$ mutant embryos (Liu et al., 2006).

Immunoprecipitation experiments confirmed these photocrosslinking and ASO-binding studies (Figure 5B). RISC was assembled with 5′ $^{32}$P-radiolabeled mm1 siRNA duplex, the mm9 duplex, or the *let-7/let-7** duplex and immunoprecipitated with anti-Ago1 monoclonal antibody; immunoprecipitated proteins were removed by digestion with protease at room temperature, and then the $^{32}$P-radiolabeled small RNAs were resolved by native gel electrophoresis to assess if they were single or double stranded. For both the mm1 siRNA duplex and the mm9 duplex, most of the Ago1-associated *let-7* was double stranded. In contrast, essentially all of the Ago1-associated *let-7* loaded from the *let-7/let-7** duplex was single stranded, indicating it had been successfully assembled into functional Ago1-RISC. Our data suggest that the conversion of pre-Ago1-RISC to mature Ago1-RISC requires additional structural features that help separate the two siRNA strands, such as mismatches in the siRNA seed

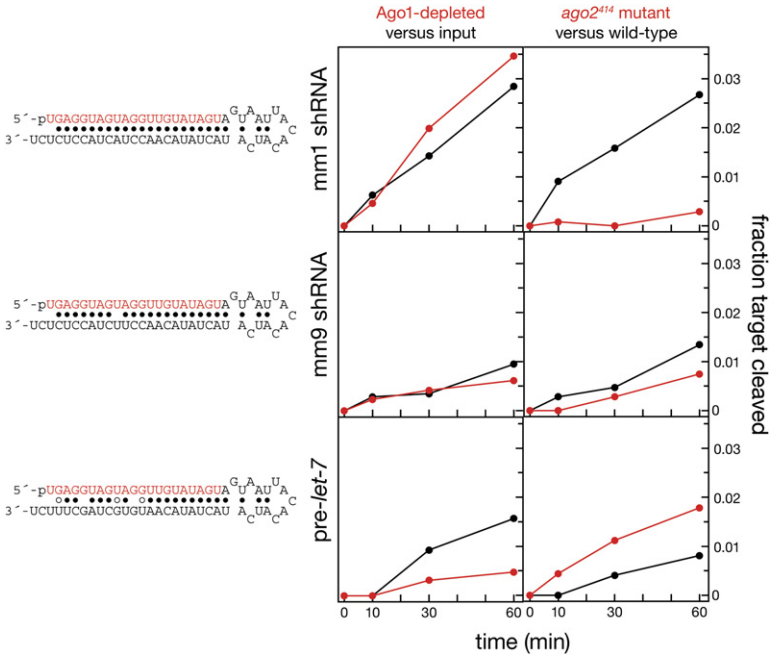


**Figure 6. The Double-Stranded Structure of Small-RNA Duplexes Generated by Dicing Longer Precursors Determines How They Are Partitioned between Ago1- and Ago2-RISC**

Two short hairpin RNAs and pre-*let-7* were incubated in embryo lysate for 1 hr to generate *let-7* by dicing and program RISC; then RISC activity in cleaving a *let-7*-complementary target RNA (0.5 nM) was measured. At left, Ago1 was immunodepleted before adding the target RNA. The red data points therefore report Ago2-RISC activity. At right, the precursors were incubated in *ago2*$^{414}$ mutant lysate, so the red data points represent only Ago1-RISC activity. For the Ago1 experiments, the precursor concentration was 20 nM; for the *ago2*$^{414}$ experiments, it was 100 nM.

region. Such features might act in a pathway similar to the "bypass" mechanism that facilitates the conversion of pre-RISC to mature RISC for Ago2 when passenger-strand cleavage is blocked (Matranga et al., 2005). In fact, when miRNA* cleavage by human Ago2 is blocked, seed mismatches between the miRNA and its miRNA* accelerate separation of the two strands (Matranga et al., 2005). We note that *Drosophila* Ago1 is more closely related to human Ago2 than to the conspecific Ago2 protein.

## Even When Small RNAs Are Diced from Longer Precursors, Their Duplex Structure Determines Small-RNA Sorting

In cells, small-RNA duplexes are produced from longer precursors by dicing. How faithfully do our studies of small-RNA sorting, which bypass this step, reflect the cellular pathway? To answer this question, we programmed *Drosophila* embryo lysate with three different Dicer substrates: (1) a short-hairpin RNA designed to generate an asymmetric *let-7* siRNA after dicing (mm1 shRNA); (2) the same shRNA, but also containing a mismatch at *let-7* position 9 (mm9 shRNA); and (3) authentic pre-*let-7* RNA. (As reported previously [Hutvágner and Zamore, 2002], less active RISC was produced in vitro from hairpin substrates than when siRNAs are used directly.)

We first incubated each precursor with embryo lysate to generate *let-7*-programmed RISC, and then we added a target RNA containing a site complementary to *let-7* and monitored target cleavage (Figure 6). Of the three precursor RNAs, mm1 shRNA produced the most active RISC. To determine the degree to which the target cleavage observed for each precursor RNA reflected Ago1-RISC programmed with *let-7*, we immunodepleted Ago1 after the RISC assembly step but before adding target RNA. Our immunodepletion strategy removed more than 98% of the Ago1 protein (Figure S6). Depletion of Ago1 reproducibly enhanced to a small extent the rate of target cleavage for mm1 shRNA, but had little effect on mm9 shRNA. In contrast, most of the RISC activity produced by pre-*let-7* was removed when Ago1 was immunodepleted. These results are consistent with mm1 shRNA loading Ago2 and pre-*let-7* loading Ago1.

To determine the degree to which the target cleavage observed for each precursor RNA reflected Ago2-RISC programmed with *let-7* (Figure 6), we compared the amount of *let-7*-directed target cleaving activity generated from each precursor in wild-type lysate to that generated in *ago2*$^{414}$ lysate, which lacks Ago2 protein. Little or no RISC activity was detected for mm1 shRNA in the *ago2*$^{414}$ mutant lysate. In contrast, for pre-*let-7* more RISC activity was detected for the *ago2*$^{414}$ mutant than for the wild-type lysate, presumably because the loss of competition with the Ago2 pathway resulted in more Ago1-RISC. As for the Ago1 immunodepletion experiment, mm9 shRNA produced less active RISC than the other two substrates. This RISC activity was reduced in the *ago2*$^{414}$ mutant lysate, consistent with our finding (Figure 5) that most of the Ago1-RISC produced by an mm9 siRNA was inactive because the siRNA remained double stranded. We conclude that dicing has little or no influence on the subsequent partitioning of a small-RNA duplex between Ago1- and Ago2-RISC.

## DISCUSSION

Here we show that in *Drosophila* the structure of a small-RNA duplex determines its partitioning between Ago1- and Ago2-RISC. Our data suggest a simple model for

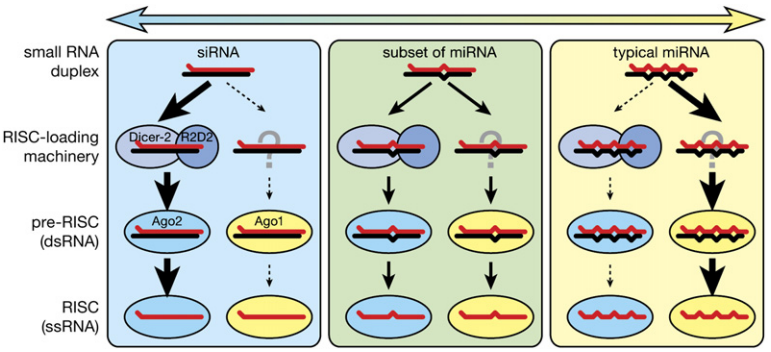


**Figure 7. A Model for Small Silencing RNA Sorting in *Drosophila***

Dcr-2/R2D2 bind well to highly paired small-RNA duplexes but poorly to duplexes bearing central mismatches; such duplexes are therefore disfavored for loading into Ago2. Ago1 favors small RNAs with central mismatches, but no Ago1-loading proteins have yet been identified. Ago1- and Ago2-loading compete each other, increasing the selectivity of small-RNA sorting. The partitioning of a small-RNA duplex between the Ago1 and Ago2 pathways reflects its structure. A typical miRNA/miRNA* duplex, such as *let-7* or *bantam*, loads mainly Ago1, whereas a standard siRNA duplex loads mostly Ago2. Some miRNA/miRNA* duplexes containing extensively paired central regions, such as miR-277/miR-277* (see Förstemann et al., 2007), partition between Ago1 and Ago2. Sorting of small-RNA duplexes into Ago1 and Ago2 produces pre-RISC, in which the duplex is bound to the Argonaute protein. Subsequently, mature RISC, which contains only the siRNA guide or miRNA strand of the original duplex, is formed. The separation of the miRNA and miRNA* or the siRNA guide and passenger strands also reflects the structure of the small-RNA duplex. For Ago1, we hypothesize that mismatches between the miRNA and the miRNA* or siRNA guide and passenger strands in the seed sequence are required for the efficient conversion of pre-RISC to mature RISC. For Ago2, such seed sequence mismatches are not needed because Ago2 can efficiently cleave the passenger or miRNA* strand, liberating the guide or miRNA from the duplex.

this partitioning (Figure 7), with a central unpaired region serving as both an antideterminant for the Ago2-loading pathway and a preferred binding substrate for the Ago1 pathway. Supporting this view, miRNAs that contain central mismatches, such as *let-7* and *bantam*, assemble primarily into Ago1-RISC (Okamura et al., 2004). The accompanying manuscript (Förstemann et al., 2007) shows that miR-277, whose central region is base paired, partitions between Ago1 and Ago2 in vivo.

Both the Ago2- and Ago1-loading pathways are selective. For Ago2, the affinity of the Dcr-2/R2D2 heterodimer for a small-RNA duplex provides the primary source of small-RNA selectivity. In the absence of either the Ago2-loading machinery or Ago2 itself, Ago1 is nonetheless preferentially loaded with a miRNA/miRNA* duplex; an siRNA duplex still loads poorly into Ago1. Thus, the Ago1-loading pathway is also inherently selective and not a default pathway that assembles small RNAs rejected by the Ago 2 pathway. We do not yet know if this selectivity is a direct property of Ago1, of an Ago1-loading machinery that remains to be identified, or both.

Previous bioinformatic analyses noted that a central region of thermodynamic instability was a common feature of miRNA/miRNA* duplexes (Khvorova et al., 2003; Han et al., 2006). Our data ascribe a function in flies to this common miRNA/miRNA* structural feature: directing the miRNA into Ago1 and away from Ago2. Mammalian miRNA/miRNA* duplexes also typically contain a central unpaired region, but it is not yet known if they are preferentially loaded into one of the four mammalian Ago-subclade Argonaute proteins.

What is the biological significance in flies of sorting miRNAs into Ago1 and siRNAs into Ago2? One idea, supported by the accompanying manuscript (Förstemann et al., 2007), is that Ago1 and Ago2 are functionally distinct, with only Ago2 silencing targets that possess extensive complementarity to the small-RNA guide and only Ago1 directing repression of targets that contain multiple but only partially complementary miRNA-binding sites. Sorting small RNAs between Ago1 and Ago2 may also prevent miRNAs from saturating the Ago2 machinery, which might compromise Ago2-mediated antiviral defense (Galiana-Arnoux et al., 2006; Obbard et al., 2006; Wang et al., 2006; Zambon et al., 2006). Conversely, excluding from Ago1 siRNAs produced in response to viral infection may minimize competition between such antiviral siRNAs and endogenous miRNAs, protecting flies from misregulation of gene expression during a viral infection. Restricting a robust RNAi—i.e., target cleavage—response to siRNAs loaded into Ago2 may also minimize undesirable, miRNA-like regulation of cellular genes by virally derived siRNAs. Thus, small-RNA sorting ensures that miRNAs are largely restricted to Ago1, whose relaxed requirement for complementarity between a miRNA and a regulated mRNA target allows each miRNA to control many different mRNAs, and that siRNAs are restricted to Ago2, whose silencing activity requires more extensive complementarity between the target and the siRNA guide.

Nonetheless, a final question remains unanswered: why do some iconoclastic miRNA/miRNA* duplexes contain features that favor their loading into Ago2?

## EXPERIMENTAL PROCEDURES

### General Methods

Preparation of 0–2 hr embryo lysate, lysis buffer, and 2x PK buffer; in vitro assembly of RISC, inactivation of RISC assembly by NEM treatment; in vitro RNAi reactions; purification of recombinant Dcr-2/R2D2 purification; and UV photocrosslinking of proteins to 5-iodo-uracil-containing siRNAs were performed as described previously (Nykanen et al., 2001; Haley et al., 2003; Tomari et al., 2004a). In vitro RNAi target cleavage was performed with 20 nM siRNA and 10 nM $^{32}$P-cap radiolabeled target RNA for Figure 3C and S4 and 0.5 nM target in Figure 6.

### 254 nm UV Photocrosslinking

20 nM 5′-$^{32}$P-labeled small-RNA duplex was incubated with lysate in a standard RNAi reaction (Haley et al., 2003) and then irradiated with 254 nM UV light for 5 min using a Stratalinker (Stratagene) with the sample ~3 cm below the UV bulbs. The photocrosslinked proteins were then resolved by 4%–20% gradient SDS-polyacrylamide gel electrophoresis (Criterion precast gels; BioRad). 2′-*O*-methyl ASO were used to isolate proteins photocrosslinked to single-stranded *let-7* as described previously (Tomari et al., 2004a).

### Ago1 Coimmunoprecipitation of Small RNAs

1 nM 5′-$^{32}$P-radiolabeled *let-7* mm11 duplex (Figure 2C) or 20 nM 5′-$^{32}$P-radiolabeled mm1, mm9, and *let-7*/*let-7** duplexes (Figure 5B) were incubated for 1 hr with wild-type embryo lysate. The reactions were then incubated with anti-Ago1 mouse monoclonal antibody (Okamura et al., 2004) tethered to Dynabeads protein G paramagnetic beads (Invitrogen) for 1 hr. The beads were washed by lysis buffer three times and the radioactivity of the bound RNA was measured by scintillation counting (Figure 2C) or the beads were deproteinized with 2 mg/ml (f.c.) proteinase K in 2x PK buffer at room temperature for 30 min, the supernatant precipitated with 2.5 volumes of absolute ethanol, and the precipitate resolved by electrophoresis in a 20% native polyacrylamide gel (19:1) containing 1x TBE and 3 mM $MgCl_2$ (Figure 5B). Control experiments demonstrated that the *let-7*/*let-7** duplex remains double stranded under these gel conditions.

Anti-Ago1 antibody beads were prepared by incubating 5 μl of tissue culture supernatant from the anti-Ago1 antibody-producing cells for every 5 μl protein G beads for 1 hr on ice and then washing the beads three times. Five microliters of these beads bearing the Ago1 antibody were used per 10–20 μl reaction.

### Native Gel Analysis of Dcr-2/R2D2:RNA and Dcr-2:RNA Complexes

Approximately 100 pM 5′-$^{32}$P-labeled small-RNA duplexes were incubated for 30 min with recombinant Dcr-2/R2D2 heterodimer or Dcr-2 alone in lysis buffer containing 5 mM DTT, 0.1 mg/ml BSA, 3% (w/v) ficoll-400, and 5% (v/v) glycerol and then resolved by electrophoresis on a 5.25% native polyacrylamide gel (37.5:1) containing 0.5x TBE and 1.5 mM $MgCl_2$. RNA and complexes were detected by phosphorimagery, quantified using an FLA-5000 image analyzer and ImageGuage 4.22 software (Fujifilm), and fit to the Hill equation with IGOR Pro 5 software (WaveMetrics).

### Ago1 Immunodepletion

For immunodepletion, 120 μl Dynabeads Protein G paramagnetic bead suspension (Invitrogen) was incubated overnight with 120 μl anti-Ago1 mouse monoclonal antibody (1B8) (Okamura et al., 2004) at 4°C with gentle agitation. Next, the magnetic beads were washed three times with lysis buffer and then split among three tubes. Each precursor RNA was incubated in 100 μl standard RNAi reaction at room temperature for 1 hr. Subsequently, 60 μl of the reaction was added to the anti-Ago1 magnetic beads, and the mixture was agitated gently at 4°C overnight. The supernatant was removed, and the beads were washed three times with lysis buffer. The input, supernatant, and beads (the immunoprecipitate) were subsequently analyzed by western blotting to confirm Ago1 depletion, by native gel analysis to measure the amount of Ago1-associated single-stranded *let-7*, and by a target cleavage assay to measure RISC activity.

### Supplemental Data

Supplemental Data include six figures and can be found with this article online at http://www.cell.com/cgi/content/full/130/2/299/DC1/.

## ACKNOWLEDGMENTS

We thank Mikiko and Haruhiko Siomi for anti-Ago1 antibody and *ago2*$^{414}$ flies, Richard Carthew for *dcr-2*$^{L811fsX}$ flies, Qinghua Liu for Dcr-2- and R2D2-expressing baculoviruses, Alicia Boucher for assistance with fly husbandry, Gwen Farley for technical assistance, and members of the Zamore lab for advice, suggestions, and critical comments on the text. P.D.Z. is a W.M. Keck Foundation Young Scholar in Medical Research. This work was supported in part by grants from the National Institutes of Health to P.D.Z. (GM62862 and GM65236) and a postdoctoral fellowship from the Human Frontier Science Program to Y.T.

Received: January 18, 2007
Revised: April 20, 2007
Accepted: May 23, 2007
Published: July 26, 2007

## REFERENCES

Baulcombe, D. (2004). RNA silencing in plants. Nature *431*, 356–363.

Bentwich, I., Avniel, A., Karov, Y., Aharonov, R., Gilad, S., Barad, O., Barzilai, A., Einat, P., Einav, U., Meiri, E., et al. (2005). Identification of hundreds of conserved and nonconserved human microRNAs. Nat. Genet. *37*, 766–770.

Bernstein, E., Caudy, A.A., Hammond, S.M., and Hannon, G.J. (2001). Role for a bidentate ribonuclease in the initiation step of RNA interference. Nature *409*, 363–366.

Berezikov, E., Guryev, V., van de Belt, J., Wienholds, E., Plasterk, R.H., and Cuppen, E. (2005). Phylogenetic shadowing and computational identification of human microRNA genes. Cell *120*, 21–24.

Berezikov, E., Thuemmler, F., van Laake, L.W., Kondova, I., Bontrop, R., Cuppen, E., and Plasterk, R.H. (2006). Diversity of microRNAs in human and chimpanzee brain. Nat. Genet. *38*, 1375–1377.

Cullen, B.R. (2004). Transcription and processing of human microRNA precursors. Mol. Cell *16*, 861–865.

Du, T., and Zamore, P.D. (2005). microPrimer: the biogenesis and function of microRNA. Development *132*, 4645–4652.

Elbashir, S.M., Lendeckel, W., and Tuschl, T. (2001a). RNA interference is mediated by 21- and 22-nucleotide RNAs. Genes Dev. *15*, 188–200.

Elbashir, S.M., Martinez, J., Patkaniowska, A., Lendeckel, W., and Tuschl, T. (2001b). Functional anatomy of siRNAs for mediating efficient RNAi in *Drosophila* melanogaster embryo lysate. EMBO J. *20*, 6877–6888.

Förstemann, K., Tomari, Y., Du, T., Vagin, V.V., Denli, A.M., Bratu, D.P., Klattenhoff, C., Theurkauf, W.E., and Zamore, P.D. (2005). Normal microRNA maturation and germ-line stem cell maintenance requires Loquacious, a double-stranded RNA-binding domain protein. PLoS Biol. *3*, e236.

Förstemann, K., Horwich, M.D., Wee, L.M., Tomari, Y., and Zamore, P.D. (2007). *Drosophila* microRNAs are sorted into functionally distinct Argonaute protein complexes after their production by Dicer-1. Cell *130*, this issue, 287–297.

Galiana-Arnoux, D., Dostert, C., Schneemann, A., Hoffmann, J.A., and Imler, J.L. (2006). Essential function in vivo for Dicer-2 in host defense against RNA viruses in *Drosophila*. Nat. Immunol. *7*, 590–597.

Griffiths-Jones, S., Grocock, R.J., van Dongen, S., Bateman, A., and Enright, A.J. (2006). miRBase: microRNA sequences, targets and gene nomenclature. Nucleic Acids Res. *34*, D140–D144.

Haley, B., and Zamore, P.D. (2004). Kinetic analysis of the RNAi enzyme complex. Nat. Struct. Mol. Biol. *11*, 599–606.

Haley, B., Tang, G., and Zamore, P.D. (2003). In vitro analysis of RNA interference in *Drosophila* melanogaster. Methods *30*, 330–336.

Hammond, S.M., Boettcher, S., Caudy, A.A., Kobayashi, R., and Hannon, G.J. (2001). Argonaute2, a link between genetic and biochemical analyses of RNAi. Science *293*, 1146–1150.

Han, J., Lee, Y., Yeom, K.H., Nam, J.W., Heo, I., Rhee, J.K., Sohn, S.Y., Cho, Y., Zhang, B.T., and Kim, V.N. (2006). Molecular basis for the recognition of primary microRNAs by the Drosha-DGCR8 complex. Cell *125*, 887–901.

Hutvágner, G., and Zamore, P.D. (2002). A microRNA in a Multiple-Turnover RNAi Enzyme Complex. Science *297*, 2056–2060.

Jing, Q., Huang, S., Guth, S., Zarubin, T., Motoyama, A., Chen, J., Di Padova, F., Lin, S.C., Gram, H., and Han, J. (2005). Involvement of microRNA in AU-rich element-mediated mRNA instability. Cell *120*, 623–634.

Khvorova, A., Reynolds, A., and Jayasena, S.D. (2003). Functional siRNAs and miRNAs exhibit strand bias. Cell *115*, 209–216.

Kim, V.N. (2005). MicroRNA biogenesis: coordinated cropping and dicing. Nat. Rev. Mol. Cell Biol. *6*, 376–385.

Kim, K., Lee, Y.S., and Carthew, R.W. (2006). Conversion of pre-RISC to holo-RISC by Ago2 during assembly of RNAi complexes. RNA *13*, 22–29.

Kloosterman, W.P., and Plasterk, R.H. (2006). The diverse functions of microRNAs in animal development and disease. Dev. Cell *11*, 441–450.

Krek, A., Grun, D., Poy, M.N., Wolf, R., Rosenberg, L., Epstein, E.J., MacMenamin, P., da Piedade, I., Gunsalus, K.C., Stoffel, M., and Rajewsky, N. (2005). Combinatorial microRNA target predictions. Nat. Genet. *37*, 495–500.

Lee, Y.S., Nakahara, K., Pham, J.W., Kim, K., He, Z., Sontheimer, E.J., and Carthew, R.W. (2004). Distinct roles for *Drosophila* Dicer-1 and Dicer-2 in the siRNA/miRNA silencing pathways. Cell *117*, 69–81.

Leuschner, P.J., Ameres, S.L., Kueng, S., and Martinez, J. (2006). Cleavage of the siRNA passenger strand during RISC assembly in human cells. EMBO Rep. *7*, 314–320.

Lewis, B.P., Shih, I.H., Jones-Rhoades, M.W., Bartel, D.P., and Burge, C.B. (2003). Prediction of mammalian microRNA targets. Cell *115*, 787–798.

Lewis, B.P., Burge, C.B., and Bartel, D.P. (2005). Conserved seed pairing, often flanked by adenosines, indicates that thousands of human genes are microRNA targets. Cell *120*, 15–20.

Liu, Q., Rand, T.A., Kalidas, S., Du, F., Kim, H.E., Smith, D.P., and Wang, X. (2003). R2D2, a Bridge Between the Initiation and Effector Steps of the *Drosophila* RNAi Pathway. Science *301*, 1921–1925.

Liu, X., Jiang, F., Kalidas, S., Smith, D., and Liu, Q. (2006). Dicer-2 and R2D2 coordinately bind siRNA to promote assembly of the siRISC complexes. RNA *12*, 1514–1520.

Matranga, C., Tomari, Y., Shin, C., Bartel, D.P., and Zamore, P.D. (2005). Passenger-strand cleavage facilitates assembly of siRNA into Ago2-containing RNAi enzyme complexes. Cell *123*, 607–620.

Nykanen, A., Haley, B., and Zamore, P.D. (2001). ATP requirements and small interfering RNA structure in the RNA interference pathway. Cell *107*, 309–321.

Obbard, D.J., Jiggins, F.M., Halligan, D.L., and Little, T.J. (2006). Natural selection drives extremely rapid evolution in antiviral RNAi genes. Curr. Biol. *16*, 580–585.

Okamura, K., Ishizuka, A., Siomi, H., and Siomi, M.C. (2004). Distinct roles for Argonaute proteins in small RNA-directed RNA cleavage pathways. Genes Dev. *18*, 1655–1666.

Pham, J.W., and Sontheimer, E.J. (2005). Molecular requirements for RNA-induced silencing complex assembly in the Drosophila RNA interference pathway. J. Biol. Chem. *280*, 39278–39283.

Pham, J.W., Pellino, J.L., Lee, Y.S., Carthew, R.W., and Sontheimer, E.J. (2004). A Dicer-2-dependent 80s complex cleaves targeted mRNAs during RNAi in *Drosophila*. Cell *117*, 83–94.

Rand, T.A., Petersen, S., Du, F., and Wang, X. (2005). Argonaute2 cleaves the anti-guide strand of siRNA during RISC activation. Cell *123*, 621–629.

Saito, K., Ishizuka, A., Siomi, H., and Siomi, M.C. (2005). Processing of pre-microRNAs by the Dicer-1-Loquacious complex in *Drosophila* cells. PLoS Biol. *3*, e235.

Schwarz, D.S., Hutvágner, G., Du, T., Xu, Z., Aronin, N., and Zamore, P.D. (2003). Asymmetry in the assembly of the RNAi enzyme complex. Cell *115*, 199–208.

Sontheimer, E.J. (2005). Assembly and function of RNA silencing complexes. Nat. Rev. Mol. Cell Biol. *6*, 127–138.

Stark, A., Brennecke, J., Bushati, N., Russell, R.B., and Cohen, S.M. (2005). Animal microRNAs confer robustness to gene expression and have a significant impact on 3′UTR evolution. Cell *123*, 1133–1146.

Tomari, Y., Matranga, C., Haley, B., Martinez, N., and Zamore, P.D. (2004a). A protein sensor for siRNA asymmetry. Science *306*, 1377–1380.

Tomari, Y., Du, T., Haley, B., Schwarz, D.S., Bennett, R., Cook, H.A., Koppetsch, B.S., Theurkauf, W.E., and Zamore, P.D. (2004b). RISC assembly defects in the *Drosophila* RNAi mutant armitage. Cell *116*, 831–841.

Tomari, Y., and Zamore, P.D. (2005). Perspective: machines for RNAi. Genes Dev. *19*, 517–529.

Valencia-Sanchez, M.A., Liu, J., Hannon, G.J., and Parker, R. (2006). Control of translation and mRNA degradation by miRNAs and siRNAs. Genes Dev. *20*, 515–524.

Wang, X.H., Aliyari, R., Li, W.X., Li, H.W., Kim, K., Carthew, R., Atkinson, P., and Ding, S.W. (2006). RNA interference directs innate immunity against viruses in adult *Drosophila*. Science *312*, 452–454.

Zambon, R.A., Vakharia, V.N., and Wu, L.P. (2006). RNAi is an antiviral immune response against a dsRNA virus in *Drosophila* melanogaster. Cell. Microbiol. *8*, 880–889.